Magnesium potassium phosphate cement: a promising binder for the conditioning of aluminum-magnesium alloys waste

Gabriel Poras, Hugo Danis, Celine Cau Dit Coumes, Pascal Antonucci, Céline Cannes, Sylvie Delpech, Stephane Perrin

Magnesium Potassium Phosphate Cement: a Promising Binder for the Conditioning of Aluminum-Magnesium Alloys Waste – 23137

G. Poras*, H. Danis*, C. Cau Dit Coumes*, P. Antonucci*, C. Cannes**, S. Delpech**, S. Perrin*
* CEA, DES, ISEC, DE2D, SEAD, LCBC, Univ Montpellier, Marcoule, France
** Université Paris-Saclay, CNRS/IN2P3, IJCLab, Orsay, France

ABSTRACT

The reprocessing of spent fuel designed for natural uranium – graphite – gas reactors has produced some waste with aluminum alloys, which need to be stabilized and solidified before their final disposal. Portland cement is extensively used for the conditioning of low-level and intermediate-level radioactive waste; however, its high alkalinity is a serious obstacle to aluminum stabilization, as it is oxidized by the mixing solution, with production of dihydrogen. This work investigates a new solution consisting in using magnesium potassium phosphate cement (MKPC) instead of Portland cement (PC). Gas chromatography and electrochemical impedance spectroscopy (EIS) are used to monitor the corrosion of pure aluminum and aluminum-magnesium alloys containing 2 to 4.5 wt.% of Mg in MKPC mortar. EIS provides qualitative information about the corrosion, but also makes it possible to assess the corrosion current using an equivalent electrical circuit linked to the kinetic parameters of the postulated corrosion mechanism. It is shown that the corrosion current of the alloys, regardless of their composition, is reduced by about two orders of magnitude in MKPC mortar as compared to Portland cement mortar. This result opens up new prospects for increasing the incorporation rate of reactive Al metal in a cementitious matrix.

INTRODUCTION

Reprocessing of spent fuel designed for natural uranium – graphite – gas (UNGG) reactors has produced some radioactive wastes containing aluminum-magnesium alloys, categorized as low-level or intermediate-level (LL-IL) radioactive wastes. These metal pieces, which were used as cartridges for transportation of the spent fuel claddings before their reprocessing (Fig. 1 left), comprise 3wt.% to 5wt.% magnesium in an aluminum matrix. They are currently stored in concrete silos at CEA Marcoule, France (Fig. 1 middle) and need to be stabilized and solidified before their final disposal (Fig. 1 right).

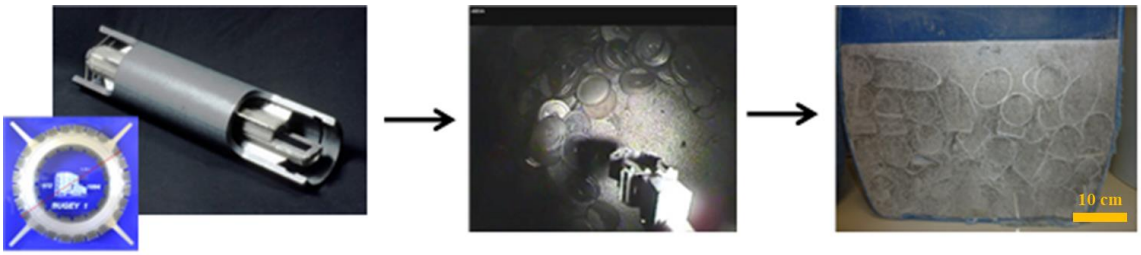

Fig. 1. UNGG fuel assembly (left); cartridges and caps made of Al−Mg alloy stored in a concrete silo (middle); aluminum pieces immobilized in a magnesium potassium phosphate cement-based material (right).

Portland cement (PC) is extensively used for the conditioning of LL-IL radioactive waste [1]; however, its high alkalinity is a serious obstacle to aluminum stabilization, this metal being oxidized by the pore solution with production of dihydrogen resulting from the reduction of water [2]. Its passivation due to the formation of a protective layer of alumina only occurs for pH values within the range 3-9 [3] (Fig. 2). Magnesium potassium phosphate cement (MKPC)-based materials, with a pore solution pH close to 8 if the Mg/P molar

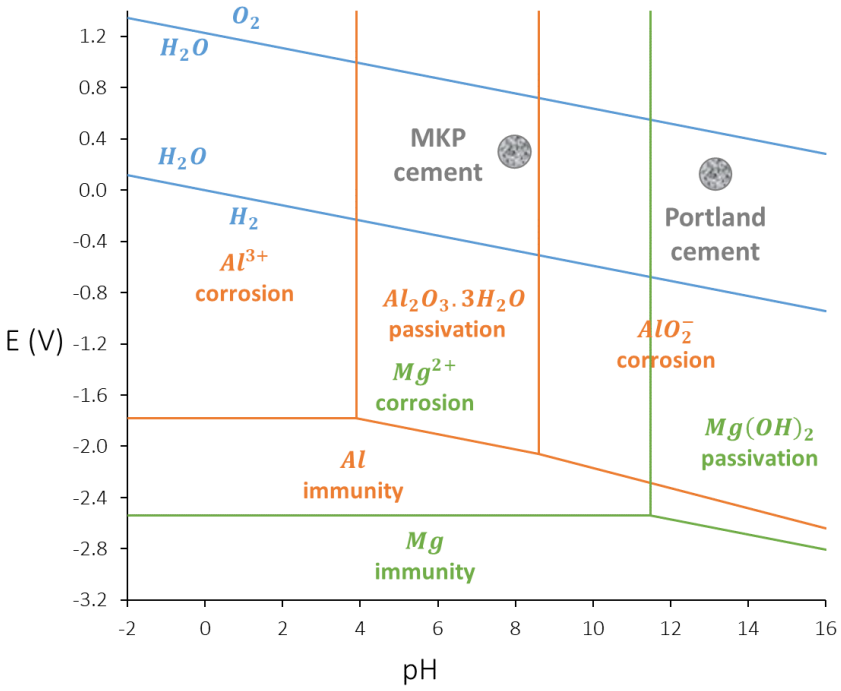

Fig. 2. E-pH diagram for pure Al (**orange**) and pure Mg (**green**) at 25°C (derived from [2], $[Al^{3+}] = [AlO_2^-] = [Mg^{2+}] = 10^{-6} mol/L$).

ratio of the cement is kept close to 1, may show better compatibility with Al metal [4]. However, this pH decrease should be detrimental to Mg metal passivation, as shown by the E-pH diagram of magnesium (Fig. 2). This work aims at investigating the corrosion of Al/Mg alloys in MKPC mortars using electrochemical impedance spectroscopy and gas chromatography to determine the evolution of the corrosion rate with ongoing hydration and its dependence on the Mg content in the alloy.

MATERIALS & METHODS

The corrosion behavior of several aluminum-magnesium alloys (Mg content varying from 0 to 4.5%wt) in a MKPC matrix is investigated using two different experimental techniques: gas chromatography and electrochemical impedance spectroscopy (EIS) at open circuit potential (OCP).

Aluminum-magnesium alloys

Different aluminum-magnesium alloys were selected for this study in order to mimick the legacy radioactive waste. Their compositions are given in TABLE I; the magnesium content in the alloy varied from 0 wt.% to 4.5 wt.%.

Al/Mg alloy	Standardized reference [5]	Al (weight %)	Mg (weight %)
Al pure		99.996 wt.%	
Al/Mg2	5251	98 wt.%	2.0 wt.%
Al/Mg3	5754	97 wt.%	3.0 wt.%
Al/Mg4.2	5086	95.8 wt.%	4.16 wt.%
Al/Mg4.5	5083	95.5wt.%	4.5 wt.%
Mg pure			99.9 wt.%

TABLE I. Compositions of Al/Mg alloys or pure metals used in this study.

The commercial alloys used in this study could have different initial surface states with significant roughness or scratches, and the presence of a native oxide layer with variable thickness. In order to remove this oxide layer, samples were immersed in a sulfuric acid solution ($[H_2SO_4] = 0.1\ mol/L$) for 30 seconds, and rinsed with demineralized water just before starting the experiments.

Design of MKPC mortar

The mix design of the mortar prepared using magnesium potassium phosphate cement is given in TABLE II. The Mg/P molar ratio and the water-to-cement weight ratio (cement = $MgO + KH_2PO_4$) were set to 1 and 0.51 respectively, which corresponded to the stoichiometry of K-struvite reaction formation [6] according to mass balance Eq. 1:

$$MgO + KH_2PO_4 + 5H_2O \rightarrow MgKPO_4.6H_2O \qquad \text{(Eq. 1)}$$

Boric acid was added as a set retarder with a $B(OH)_3$-to-cement weight ratio set to 0.02 [7]. Low-CaO content coal fly ash and sand were added with a weight ratio of 1 compared to cement. Details on the composition and physical properties of the raw materials are given in the work of Chartier et al [8] (fly ash: Cordemais 2013).

Raw constituents	Weight (g)
MgO	129.4
KH_2PO_4	437.1
water	289.0
fly ash	566.6
sand	566.6
H_3BO_3	11.3

TABLE II. Mix design of MKPC mortar (for 2kg ~ 1L batch).

Gas analysis

Gas chromatography was used to monitor the production of hydrogen due to the corrosion process. Indeed, as aluminum and magnesium are oxidized, water is reduced, which produces hydrogen, as shown by the following reactions:

$$Al + 3H_2O \rightarrow Al^{3+} + {}^{3}/_{2}\,H_2 + 3OH^- \qquad (Eq.\ 2)$$

$$Mg + 2H_2O \rightarrow Mg^{2+} + H_2 + 2OH^- \qquad (Eq.\ 3)$$

Samples made of metal pieces with a total surface area of $200\ cm^2$ were embedded in $100\ mL$ fresh MKPC mortar in a polyethylene cell; the cell was introduced in an airtight stainless steel reactor, as shown in Fig. 3. The reactor was placed under nitrogen atmosphere using a vacuum pump and a nitrogen supply. The H_2 gas released in the headspace of the reactor was analyzed by gas chromatography after periods of time ranging from 1 day to 8 months and its content was standardized with respect to the surface area of metal in contact with the mortar.

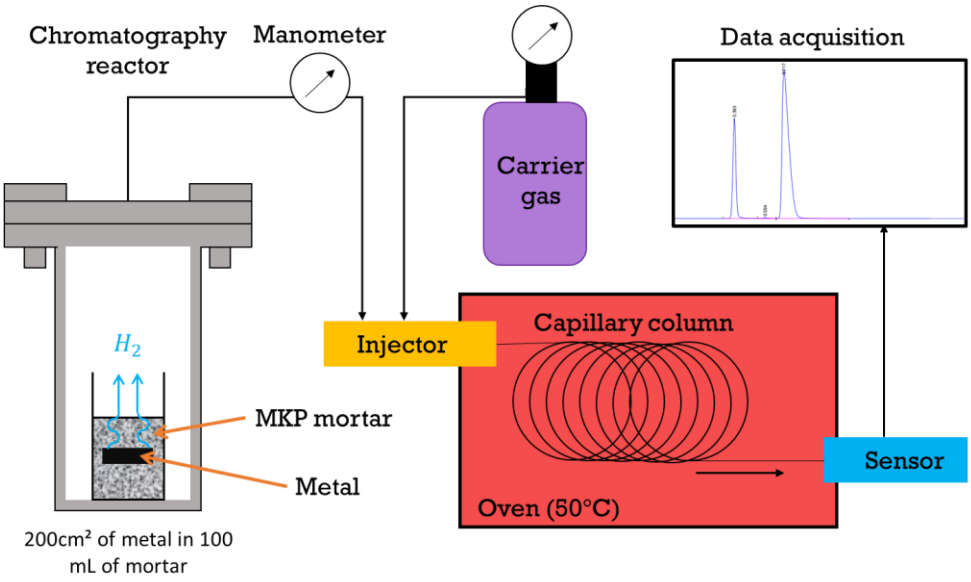

Fig. 3. Monitoring of the gas released by the mortar samples encapsulating Al/Mg alloys by gas chromatography.

Electrochemical characterizations

For the electrochemical experiments, a specific cell was designed (Fig. 4), comprising 4 electrodes (1 in Al/Mg alloy and 3 in Pt) embedded in the cement matrix, and making it possible to get information both on the corrosion of the Al/Mg metal [9] and on the evolution of the matrix over time by using the inert platinum electrodes [10]. The open circuit potential (OCP) was first measured. The impedance spectrum of the system was then acquired at OCP by applying a small sinusoidal potential disturbance $\Delta E(\omega)$ (amplitude 10 mV) between the working and the reference electrodes, with a frequency varying from 0.1 to 10^7 Hz (10 points per decade), and measuring the resulting current variation $\Delta I(\omega)$ going through the working and counter electrodes. The impedance of the system was defined as: $Z(\omega) = \Delta E(\omega)/\Delta I(\omega)$.

The potential disturbance was applied on the platinum inert working electrode to study the matrix properties, and on the Al/Mg alloy working electrode for the corrosion study. Between two measurements, the samples were cured at room temperature. The tightly closed cells prevented any desiccation of the mortar.

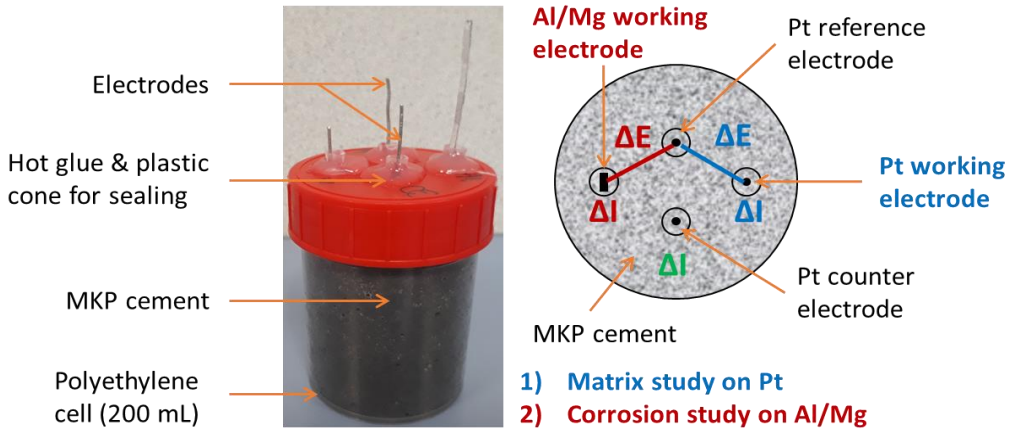

Fig. 4. Impedance spectroscopy on Al/Mg alloys embedded in MKPC mortar: experimental cell (left) & position of the electrodes (right).

RESULTS & DISCUSSION

H_2 release

Fig. 5 shows the H_2 release by the different samples. The cumulative volume of gas ranged between 0.4 and 0.5 L/m^2 after 230 days for the different Al/Mg alloys. Note that the experimental error was important, for instance close to $\pm$ 0.12 L/m^2 for Al/Mg3 alloy at 230 days. At a given characterization time, the variations observed for the different alloys were of the same magnitude as the experimental error and were thus considered as non-significant. Consequently, the H_2 release did not seem to be influenced by the Al alloy grade. It remained much lower than that measured when pure magnesium was embedded in MKPC mortar (more than 3 L/m^2 at 230 d - curve not shown here). Besides, the gas release when pure aluminum was encapsulated in a Portland cement paste reached 40 L/m^2 in only 4 hours [2]. These results thus confirm that MKPC seems more adapted than PC for the conditioning of pure Al, but also of Al alloys containing small amounts of magnesium.

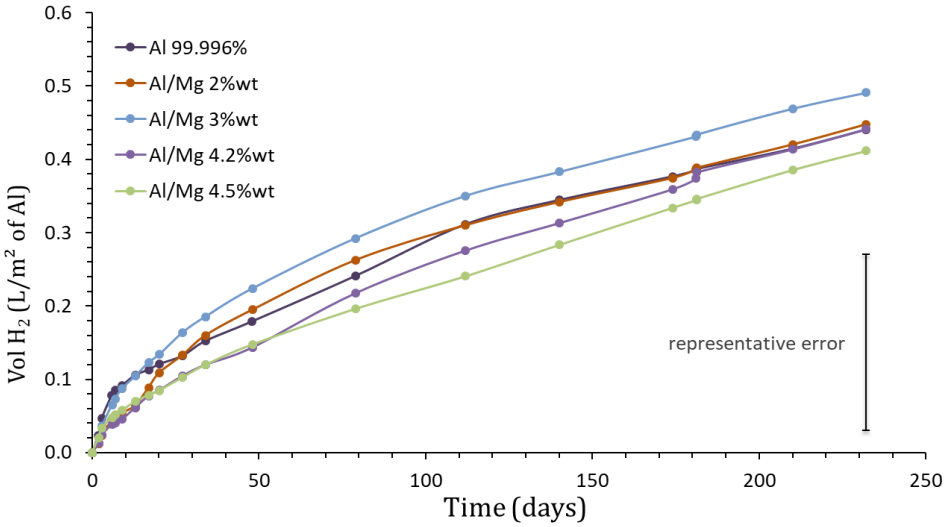

Fig. 5. Normalized H_2 production as a function of the alloy grade (P = 1 atm, T = 25°C).

Electrochemical results

Impedance spectra acquired on the different Al/Mg alloys embedded in MKPC mortar after 6 days of curing are shown in Fig. 6. Since the measured impedance Z inversely depended on the electrode surface area S [9], the corrected impedance $Z \times S$ was plotted on Nyquist and Bode diagrams in order to compare data obtained with electrodes having different surface areas.

The small impedance values, measured at high frequencies (Fig. 6) mainly resulted from the mortar contribution. On the contrary, the high impedance values measured at t low frequencies were linked to the corrosion process. The Nyquist diagrams at low frequency could be qualitatively analyzed as follows: the more vertical the plot the slower the corrosion rate. Therefore, after 6 days of curing, corrosion of Al was slower than that of Mg in the MKPC mortar, as expected from the E-pH diagrams. Al/Mg alloys had corrosion rates intermediate between those of Al and Mg.

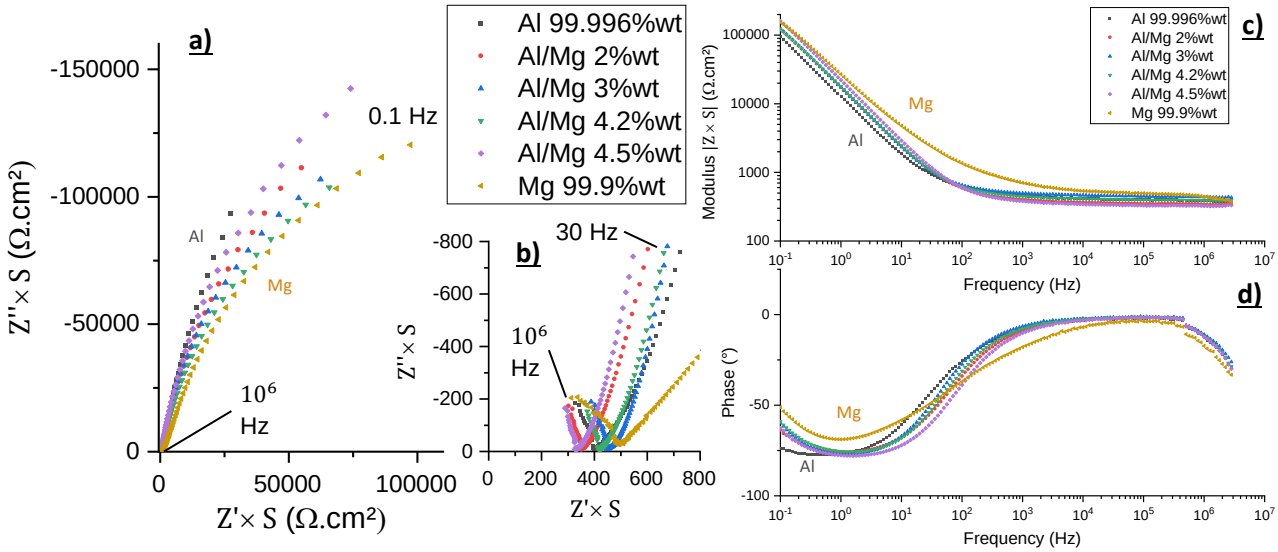

Fig. 6. Experimental impedance spectra of Al/Mg alloys embedded in magnesium-potassium phosphate cement after 6 days of curing at 20°C. a) Nyquist plot - b) Zoom at high frequencies - c) and d) Bode modulus and phase plots.

The spectrum recorded for pure magnesium at high frequency was quite different. This could result from the higher H_2 production that may change the properties of the MKPC mortar, such as its porosity. At intermediate frequencies, a straight line with a phase angle of 45° was observed, which was characteristic of a diffusion impedance.

This qualitative analysis was complemented by analyzing the evolution of the open circuit potential (OCP) measured on the different Al/Mg alloy electrodes as a function of time. OCP was measured versus a platinum reference electrode embedded in the MKPC mortar. The OCP values presented in Fig. 7 were compared to the cathodic limit of water in the cementitious matrix. This latter was determined using cyclic voltammetry on Pt electrode, and was found to be close to $-0.9V/Pt$. Therefore, the high corrosion zone in MKPC mortar corresponded to OCP values below $-0.9V/Pt$ (grey zone in Fig. 7).

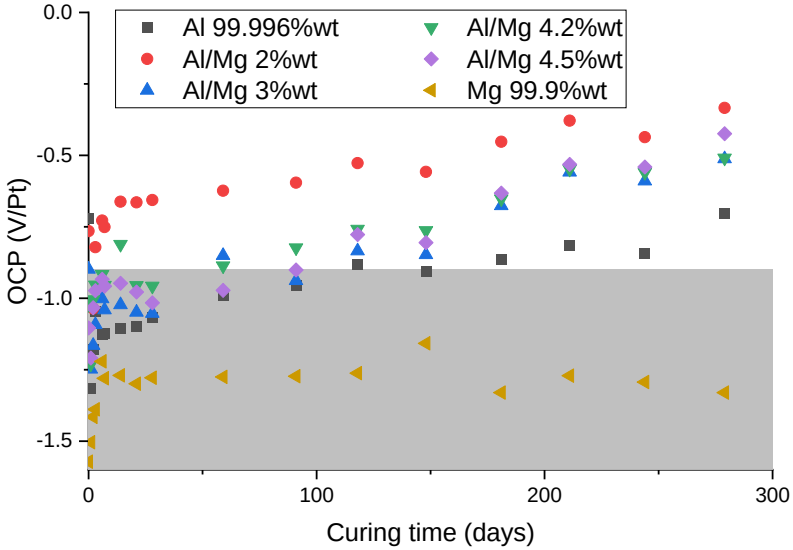

Fig. 7. Variation of OCP measured on different Al/Mg alloy electrodes vs platinum electrode as a function of time. Grey zone = “high corrosion zone”.

Whatever the investigated Al/Mg alloy, the OCP value decreased a lot between day 0 (fresh mortar) and day 1 (hardened material). Then, until 6 days of curing, the OCP increased quickly. A slowing down was noticed after 6 days, except for pure Mg. The OCP value of all the Al and Al/Mg alloys exceeded the cathodic limit after a certain curing time (almost 100 days for pure Al), which indicated that corrosion stopped, likely due to the formation of a passivation layer of alumina. Oppositely, pure Mg was continuously corroded throughout the course of the study as its OCP stayed in the corrosion zone of MKPC mortar.

In order to investigate more thoroughly the corrosion mechanism of Al metal and Al alloys, a quantitative analysis based on EIS was performed. The objective was twofold:

- model the impedance spectra to assess the kinetic parameters of the corrosion process for the different metals,
- compare the H_2 release inferred from the corrosion rate determined by EIS to that measured experimentally by gas chromatography to check the consistency of the two approaches.

To model the impedance spectra, it is necessary to take into account the cement matrix contribution to the impedance, and the faradic impedance linked to the corrosion mechanism.
Song et al (2000) [10] have described the cement mortar contribution to the impedance by distinguishing different conductive paths (Fig. 8):

- the "insulator" conductive path (ICP) through the hydrates is modelled by a pure capacitance C_m,
- the continuous conductive path (CCP) through the open porosity and the electrolyte is modelled by a pure resistance R_e,
- discontinuous conductive paths (DCP) through the closed porosity of the matrix are modelled by using a resistance and a capacitance in series.

In MKPC matrix, it is necessary to consider two DCP in parallel to fit the experimental results; this is attributed to the progressive development of the pore network.

As the metallic electrode is immersed in the MKPC mortar, an electrical double layer of ions is formed at the interface between the conductive electrode and the electrolyte; this phenomenon is represented by a constant phase element CPE_{dc}, which is in parallel with the faradaic impedance accounting for corrosion.

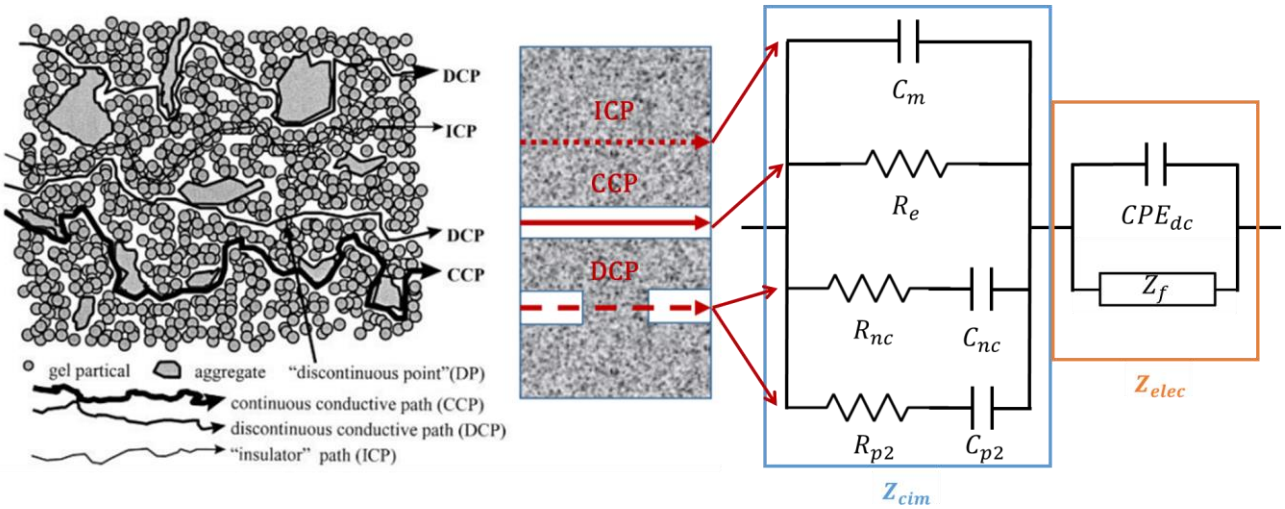

Fig. 8. Conductive paths through the microstructure of concrete (left), as described by Song et al (2000) [10]; schematic representation and equivalent electrical circuit used in this study (right).

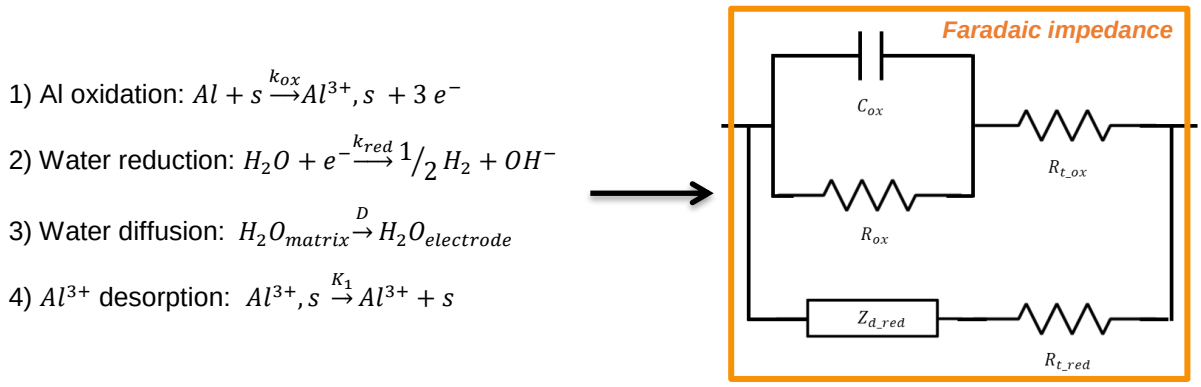

Fig. 9. Postulated electrochemical mechanism of the corrosion process in the cement matrix (left) and calculated equivalent electrical circuit (right).

An electrochemical mechanism in four stages was postulated to describe the corrosion process, taking into account water diffusion, Al^{3+} diffusion and passivation by precipitation of Al_2O_3 (Fig. 9). An equivalent electrical circuit was then derived from this mechanism using Fick's law and Butler-Volmer equation; the calculation method can be found in Delpech et al (2017) [9].

All the electrical parameters in Fig. 9 were expressed as a function of the kinetic parameters of the Al corrosion mechanism. The electrical parameters were adjusted by fitting the impedance spectra recorded after increasing periods of curing using a homemade Python™ fitting script.

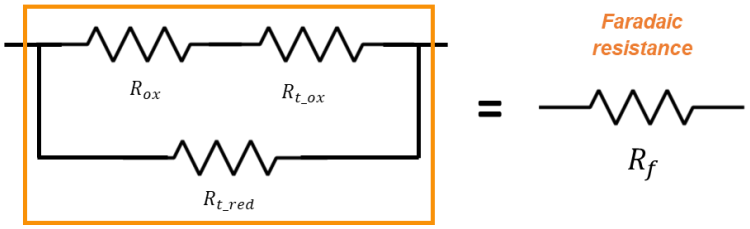

Fig. 10. Simplified equivalent electrical circuit of the faradaic impedance for Al and Al/Mg alloys in MKPC mortar.

Fitting of the various spectra showed that the faradaic impedance could be simplified for Al and Al/Mg alloys by neglecting the Z_{d_red} and C_{ox} elements. Indeed, the impedance spectra of this metals did not show any contribution of water diffusion (resulting from a straight line with a slope at 45° on Nyquist diagram), and the diffusion parameters could be varied over a large domain without any influence on the modelled spectra. Secondly, the C_{ox} capacitance was very low due to the passivation of the electrode (C_{ox}~$10^{-13}F$) and was thus negligible compared to the double-layer capacitance CPE_{dc} (C_{dc}~$10^{-5}F$). Consequently, the faradaic impedance comprised three resistances, which were equivalent to a pure faradaic resistance R_f (Fig. *10*).

Fig. 11 compares the experimental and calculated spectra for pure aluminum encapsulated in MKPC mortar. The simulated spectra using the electrical circuit shown in Fig. 8 and a pure faradaic resistance rather well fitted the experimental data. Two main changes occurred over time on the Nyquist diagram: firstly, at high frequencies/low impedance values (zoom on the Fig. 11-left), the matrix contribution to the impedance evolved during hydration, with an increase of the electrolyte resistance. Secondly, the impedance at low frequencies increased over time, and the shape of the Nyquist diagram became almost vertical, meaning that corrosion was slowing down.

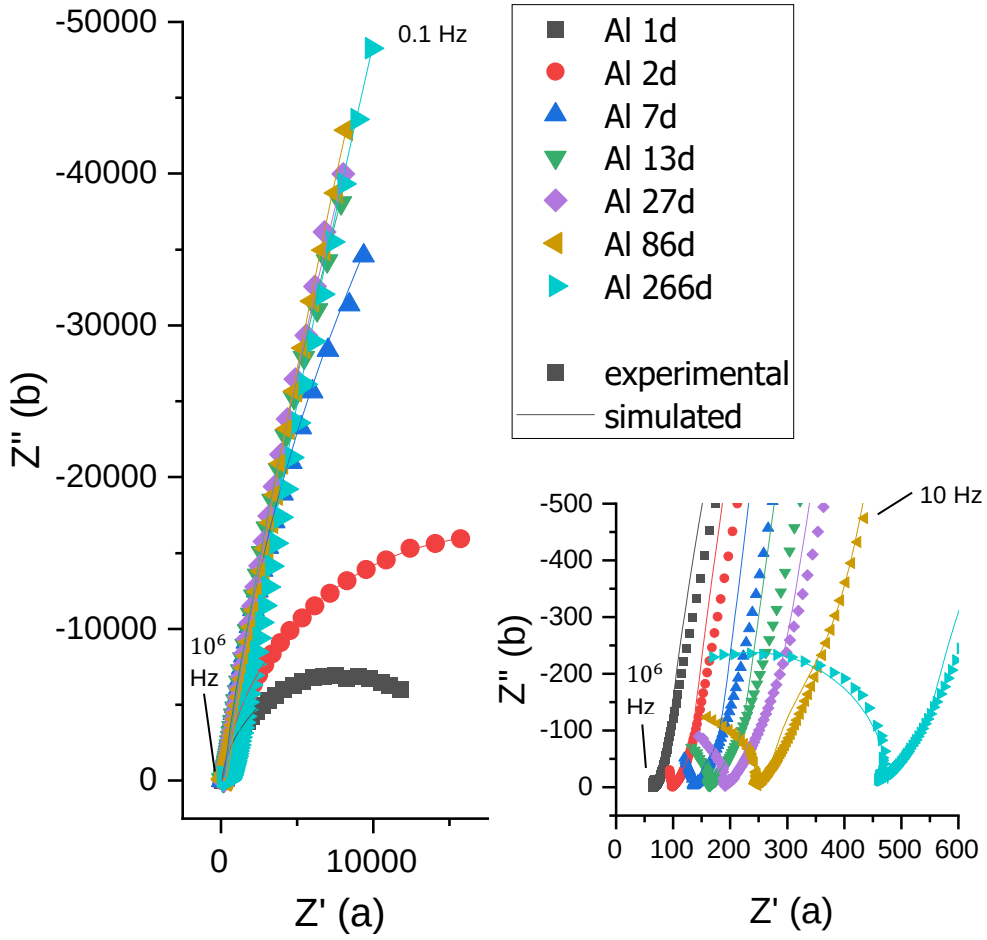

Fig. 11. Experimental and simulated impedance spectra of pure Al embedded in MKPC mortar after increasing curing times at 20°C.

The corrosion current I_{corr} and the equivalent hydrogen release by unit of surface $V_{H_2/S}$ were then calculated from the fitted faradaic resistance value R_f using the following equations:

$$I_{corr} = \frac{RT}{\alpha_{red} F * R_f} \qquad (Eq. 4)$$

$$V_{H_2/S}(t) = \frac{RT}{P} * \frac{3}{2} * \frac{1}{3FS} * \int_0^t I_{corr} \qquad (Eq. 5)$$

with R the molar gas constant, T the temperature, F the Faraday constant, P the pressure, S the surface area of the electrode and α_{red} the charge transfer coefficient for water reduction. Fig. 12 compares the evolution of the faradaic resistance and corrosion current obtained for the different aluminum grades. In all cases, the faradaic resistance increased quickly during the first days of hydration; inversely, the corrosion current decreased from $\sim 10^{-5}\ A$ at 1 day to $\sim 10^{-7}\ A$ or less at 27 days. Corrosion thus slowed down by at least 2 orders of magnitude with ongoing cement hydration. This could either result from metal passivation, but also from a lack of water available in the MKPC mortar for the corrosion process since water was progressively depleted by cement hydration. Besides, the corrosion current for pure aluminum encapsulated in a Portland cement paste decreased to $\sim 5 * 10^{-6}\ A$ after 150 days [9]; the corrosion current for pure aluminum in a MKPC mortar is close to $5 * 10^{-8}\ A$ (Fig. 12) at the same hydration state. This decrease of

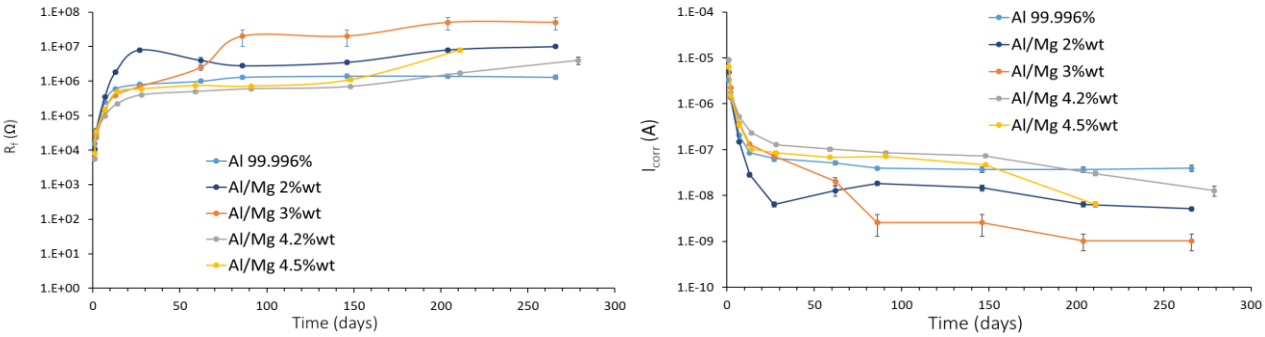

Fig. 12. Evolution of the faradaic resistance R_f and corrosion current I_{corr} derived from fitting of the EIS spectra for Al and Al/Mg alloys embedded in MKPC mortar.

long term corrosion current by almost two orders of magnitude confirms that MKPC seems more adapted than PC for the conditioning of pure Al.

The corrosion current could not be simply correlated to the Mg content of the alloy. At early age, all alloys yielded close corrosion current values, whereas at later age, differences by more than one order of magnitude were observed. At 266 days, the smallest and highest corrosion current values were recorded for Al/Mg3 ($\sim 10^{-9}\ A$) and pure Al ($\sim 4.10^{-8}\ A$) respectively. The experimental error on the corrosion current derived from fitting was comprised between 10% to 40% and could not be the single factor explaining the differences observed between alloys.

Discussion

Knowing the corrosion current, it was possible to calculate an equivalent hydrogen release (standardized with respect to the metal surface area) using Eq. 5. This calculated release was compared to that determined experimentally using gas chromatography (Fig. 13). At first sight, the two sets of data were of the same magnitude order, which tended to validate the quantitative analysis of EIS spectra developed in this study.

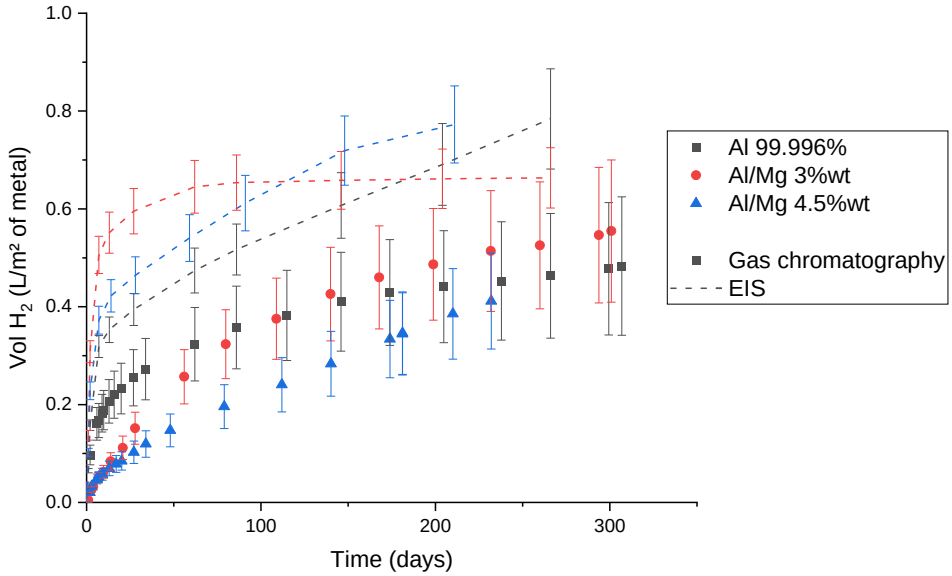

Fig. 13. Comparison of the equivalent hydrogen release by surface area of metal obtained by gas chromatography and EIS (P = 1 atm, T = 25°C).

However, the H_2 production derived from EIS systematically exceeded that measured by GC, the difference between the two techniques being more important at early age than at later age. This could result from two factors. On one hand, the hydrogen produced in the MKPC mortar during the corrosion process may be to some extent confined in the mortar, either trapped in the closed porosity or dissolved into the pore solution. Consequently, the H_2 released in the headspace of the reactor would only represent a fraction of the H_2 produced by corrosion. With time, this trapped gas may diffuse through the mortar, explaining the better agreement between GC and EIS results in the long term. On the other hand, the calculation of the equivalent H_2 release from the corrosion current assumes that the only oxidation process occurring is aluminum oxidation, and that it produces hydrogen. This is not fully true since oxidation of magnesium should also be taken into account for Al/Mg alloys. Magnesium is present at a low content in the alloys, but it is more corroded than aluminium under the near neutral pH conditions set by the MKPC mortar. Besides, other oxidation routes, for instance involving dissolved oxygen, may occur without any hydrogen production.

As previously shown by the GC results, the cumulative H_2 release calculated from the corrosion current did not significantly depend on the Mg content in the alloy. The differences noted on the corrosion current values after one month had very limited influence on the cumulative gas production, which could be explained by the fact that, whatever the investigated metal, its corrosion current was reduced by several orders of magnitude after one month. Corrosion occurring at early age had thus a dominating contribution to the cumulative H_2 release. Moreover, EIS is a punctual method allowing to measure corrosion current at a given time, which is then integrated to calculate the cumulative H_2 release, whereas GC directly measures the cumulated gas produced by corrosion. Corrosion current calculated by EIS was considered to evolve linearly between two measures, which is a hypothesis potentially leading to an experimental error on the H_2 release.

CONCLUSIONS

The main conclusions of this work can be summarized as follows:

- EIS is a non-destructive technique well adapted to monitor the corrosion of metals in a cementitious material,
- Using MKPC instead of PC strongly mitigates the corrosion of Al/Mg alloys,
- The Mg content in the Al alloy has limited influence on the cumulative H_2 production resulting from corrosion.

Therefore, magnesium phosphate cement may be considered as a promising binder for the conditioning of deleterious radioactive waste containing aluminum and aluminum-magnesium alloys. Nevertheless, in the long term, resaturation of the cement matrix by groundwater in the repository cannot be excluded. Its influence on metal corrosion should thus be assessed : it could indeed lead to an evolution of the corrosion process due to the renewed presence of water and/or hydrolysis of the cement matrix.

REFERENCES

[1] F. Bart, C. Cau-dit-Coumes, F. Frizon, S. Lorente, Cement-based materials for nuclear waste storage, Springer Science & Business Media, 2012.
[2] C. Cau Dit Coumes, D. Lambertin, H. Lahalle, P. Antonucci, C. Cannes, S. Delpech, Selection of a mineral binder with potentialities for the stabilization/solidification of aluminum metal, J. Nucl. Mater. 453 (2014) 31–40.
[3] M. Pourbaix, Atlas d'équilibres électrochimiques, 1963.
[4] H. Lahalle, Conditionnement de l'aluminium métallique dans les ciments phospho-magnésiens, Thèse, Université de Bourgogne Franche-Comté, 2016.
[5] Aluminum Association, International Alloy Designations and Chemical Composition Limits for Wrought Aluminum and Wrought Aluminum Alloy, 2018.
[6] B. Xu, H. Ma, H. Shao, Z. Li, B. Lothenbach, Influence of fly ash on compressive strength and micro-characteristics of magnesium potassium phosphate cement mortars, Cem. Concr. Res. 99 (2017) 86–94.
[7] H. Lahalle, C. Cau Dit Coumes, C. Mercier, D. Lambertin, C. Cannes, S. Delpech, S. Gauffinet, Influence of the w/c ratio on the hydration process of a magnesium phosphate cement and on its retardation by boric acid, Cem. Concr. Res. 109 (2018) 159–174.
[8] D. Chartier, J. Sanchez-Canet, P. Antonucci, S. Esnouf, J.-P. Renault, O. Farcy, D. Lambertin, S. Parraud, H. Lamotte, C.C.D. Coumes, Behaviour of magnesium phosphate cement-based materials under gamma and alpha irradiation, J. Nucl. Mater. 541 (2020) 152411.
[9] S. Delpech, C. Cannes, N. Barré, Q.T. Tran, C. Sanchez, H. Lahalle, D. Lambertin, S. Gauffinet, C.C.D. Coumes, Kinetic Model of Aluminum Behavior in Cement-Based Matrices Analyzed by Impedance Spectroscopy, J. Electrochem. Soc. 164 (2017) C717–C727.
[10] G. Song, Equivalent circuit model for AC electrochemical impedance spectroscopy of concrete, Cem. Concr. Res. 30 (2000) 1723–1730.